

Comparative Time-Resolved Photosystem II Chlorophyll *a* Fluorescence Analyses Reveal Distinctive Differences between Photoinhibitory Reaction Center Damage and Xanthophyll Cycle-Dependent Energy Dissipation*

Adam M. Gilmore^{1,2}, Theodore L. Hazlett^{3,4}, Peter G. Debrunner^{4,5} and Govindjee†^{1,5}

¹Department of Plant Biology, UIUC, Urbana, IL, USA;

²Photobioenergetics Group, ANU/RSBS, Canberra, Australia;

³Laboratory for Fluorescence Dynamics;

⁴Department of Physics and ⁵Center for Biophysics and Computational Biology, UIUC, Urbana, IL, USA

Received 4 March 1996; accepted 4 June 1996

ABSTRACT

The photosystem II (PSII) reaction center in higher plants is susceptible to photoinhibitory molecular damage of its component pigments and proteins upon prolonged exposure to excess light in air. Higher plants have a limited capacity to avoid such damage through dissipation, as heat, of excess absorbed light energy in the PSII light-harvesting antenna. The most important photoprotective heat dissipation mechanism, induced under excess light conditions, includes a concerted effect of the trans-thylakoid pH gradient (ΔpH) and the carotenoid pigment interconversions of the xanthophyll cycle. Coincidentally, both the photoprotective mechanism and photoinhibitory PSII damage decrease the PSII chlorophyll *a* (Chl *a*) fluorescence yield. In this paper we present a comparative fluorescence lifetime analysis of the xanthophyll cycle- and photoinhibition-dependent changes in PSII Chl *a* fluorescence. We analyze multifrequency phase and modulation data using both multicomponent exponential and bimodal Lorentzian fluorescence lifetime distribution models; further, the lifetime data were obtained in parallel with the steady-state fluorescence intensity. The photoinhibition was characterized by a progressive decrease in the center of the main fluorescence lifetime distribution from ~ 2 ns to ~ 0.5 ns after 90 min of high light exposure. The damaging effects were consistent with an increased nonradiative decay path for the charge-separated state of the PSII reaction center. In contrast, the ΔpH and xanthophyll cycle had concerted minor and major effects, respectively, on the PSII fluorescence lifetimes and intensity (Gilmore *et al.*, 1996, *Photosynth. Res.*, in press). The minor change decreased both the width and lifetime center of the longest lifetime distribution; we suggest that

this change is associated with the ΔpH -induced activation step, needed for binding of the deepoxidized xanthophyll cycle pigments. The major change increased the fractional intensity of a short lifetime distribution at the expense of a longer lifetime distribution; we suggest that this change is related to the concentration-dependent binding of the deepoxidized xanthophylls in the PSII inner antenna. Further, both the photoinhibition and xanthophyll cycle mechanisms had different effects on the relationship between the fluorescence lifetimes and intensity. The observed differences between the xanthophyll cycle and photoinhibition mechanisms confirm and extend our current basic model of PSII exciton dynamics, structure and function.

INTRODUCTION

Plants have evolved biochemical and biophysical mechanisms to adapt and protect themselves against excess light in their environment (1–4). The research in this area has focused on the following two different mechanisms that serve a similar function, if not purpose, that being to decrease the efficiency of the photochemical reactions of photosystem II, PSII.‡ The first mechanism dissipates excess

*The authors dedicate this paper, with their best wishes, to honor Professor Horst Senger's 65th birthday.

†To whom correspondence should be addressed at: Department of Plant Biology, University of Illinois at Urbana–Champaign, 265 Morrill Hall, 505 S. Goodwin Ave., Urbana, IL 61801-3707, USA. Fax: (217) 244-7246; e-mail: gov@uiuc.edu; <http://www.life.uiuc.edu/govindjee/>

© 1996 American Society for Photobiology 0031-8655/96 \$5.00+0.00

‡Abbreviations: A, antheraxanthin; BSA, bovine serum albumin; c_x , lifetime center of fluorescence lifetime component *x*; Chl *a*, *b*, chlorophyll *a*, *b*; CP, chlorophyll binding protein of photosystem II inner antenna; DCMU, 3-(3,4-dichlorophenyl)-1,1-dimethylurea; f_x , fractional intensity of fluorescence lifetime component *x*; F_m , F'_m , maximal fluorescence intensity with all Q_A reduced in the absence, presence of nonphotochemical quenching; F_{m_i} , maximal fluorescence intensity in the presence of photoinhibitory nonphotochemical quenching; F_{m_o} , minimal fluorescence intensity with all Q_A oxidized; LHCIIb, main light-harvesting pigment–protein complex (of photosystem II); PAM, pulse-amplitude modulation fluorometer; PFD, photon flux density; PSI, photosystem I; PSII, photosystem II; P680, special pair of chlorophylls of PSII reaction center; Q_A , primary quinone electron acceptor of PSII; V, violaxanthin; w_x , width at half maximum of Lorentzian distribution component *x*; Z, zeaxanthin; ΔpH , trans-thylakoid membrane proton gradient; $\langle\tau\rangle$, $\langle\tau\rangle' = \sum c_x f_x$, average lifetime of Chl *a* fluorescence in the absence, presence of nonphotochemical fluorescence quenching; τ_f , lifetime of chlorophyll *a* fluorescence from PSII.

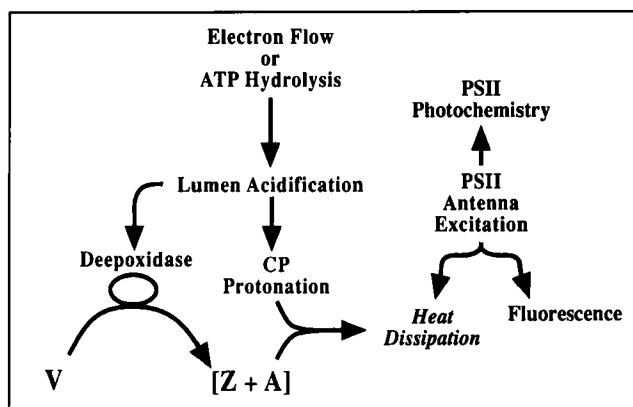


Figure 1. Control of the antenna-mediated heat dissipation in the PSII antenna by photosynthetic events at the thylakoid membrane level. Figure modified from Gilmore *et al.* (6).

absorbed light energy as heat in the light-harvesting processes of the PSII antennae complexes and involves special carotenoid pigments of the xanthophyll cycle (4–6); this mechanism is to be referred to as the xanthophyll cycle-dependent mechanism. The second mechanism converts the PSII reaction center into a heat-dissipating center with a low photochemical yield and primarily involves oxidative molecular degradation of the component pigments and proteins of the reaction center; this mechanism is to be referred to as the aerobic photoinhibition mechanism (7–10). It should be noted that although excessive illumination under anaerobic conditions also inhibits PSII function, anaerobic photoinhibition effects are of a different biochemical nature than those observed under the aerobic conditions of this and other studies (10–13); anaerobic conditions were not explored in this paper.

Even though the xanthophyll-cycle and aerobic photoinhibition mechanisms are mediated by different biochemical changes, both are elicited in response to the absorption of excess photons by the photosynthetic apparatus. Because both mechanisms dissipate light energy as heat in the photosynthetic apparatus both also decrease (quench) the yield of PSII chlorophyll (Chl) *a* fluorescence. Therefore, PSII fluorescence serves as a useful tool for quantifying the effects of these mechanisms on the PSII photochemical apparatus; for a review of PSII reactions, see Diner and Babcock (14), and for a discussion on its fluorescence, see Govindjee (15). With respect to this paper it is important to note that the xanthophyll cycle and photoinhibition mechanisms are normally elicited in response to highly contrasting levels of excess absorbed light. The xanthophyll cycle-dependent mechanism generally responds to much lower and variable levels of excess light (2,4), whereas the aerobic photoinhibition mechanism is normally observed after prolonged and very extreme excess light conditions (2,7,10). Indeed, studies of aerobic photoinhibition often involve light intensities and exposures far above those that would ever be experienced by a plant under natural or physiological conditions (8–13,16).

It follows that the different sensitivity of the xanthophyll cycle and photoinhibition mechanisms to excess light is attributable to their different biochemical mechanisms. As shown schematically in Fig. 1, the xanthophyll cycle mechanism is under complex influence of photosynthetic events

at the thylakoid membrane level but is primarily controlled by the trans-thylakoid pH gradient, ΔpH (6). The acidification of the thylakoid lumen is believed to play two roles in the xanthophyll cycle mechanism. First, the lumen pH activates the xanthophyll cycle deepoxidase enzyme (17), which converts the diepoxide violaxanthin (V) to zeaxanthin (Z) via the monoepoxide intermediate antheraxanthin (A) (18). Second, the lower lumen pH protonates carboxyl residues at the luminal side of the minor light-harvesting complexes of PSII, namely, CP26 and CP29 (5,19–21). Bassi *et al.* (22) showed that the minor CP26 and CP29 proteins were enriched in the xanthophyll cycle pigments. Thus, it was suggested that upon protonation of the minor CP proteins, a special binding interaction is stimulated between the minor CP proteins and both the Z and A molecules (6,22,23); the special interaction of these xanthophylls with the CP proteins then results in an increased rate constant of heat dissipation within the PSII antenna processes. The increased heat dissipation competes with other pathways of antenna de-excitation, decreasing the quantum yields of both the PSII photochemistry and the fluorescence.

The primary aerobic photoinhibitory damage is believed to be associated with singlet-oxygen- and oxygen-radical-mediated degradation of the P680 Chl and protein components of the PSII reaction center (see *e.g.* 8–13). The main protein that is damaged and degraded in this process is the D1 protein, but damage to the D2, CP43 and CP29 proteins has also been implicated (see *e.g.* 10,11,16). One of the major consequences of photoinhibition is a block in electron transport on the acceptor side of the PSII reaction center, the details of which are still being investigated. The cause of the PSII Chl *a* fluorescence quenching during photoinhibitory light treatment in air is also still being investigated. Recent time-resolved (9,12) and steady-state (13) studies of PSII Chl *a* fluorescence suggest that quenching by aerobic photoinhibition is due to an effect on the primary charge-separated state of the PSII reaction center; this effect may increase the rate constant for a nonradiative decay pathway from the charge-separated state. Kirilovsky *et al.* (13) suggest that aerobic photoinhibition is a more complex sequence of events involving modification of the acceptor-side reactions of PSII, overreduction of the primary quinone electron acceptor of PSII (Q_A) and overoxidation of the donor-side of PSII; the fluorescence quencher may be an oxidizing species such as a Chl⁺ cation or the P680⁺ cation (9,24–26). Although, the early stages of photoinhibition may involve impaired function of Q_A and formation of doubly reduced Q_A^{2-} , Vass *et al.* (26) concluded that Q_A^{2-} does not accumulate in response to prolonged aerobic photoinhibition and thus is not responsible for the fluorescence quenching (27,28).

As discussed above, and because it is clear that the xanthophyll cycle and photoinhibition PSII Chl *a* fluorescence quenching mechanisms are due to different biochemical changes, it was of paramount interest to determine and compare their effects on the PSII Chl *a* fluorescence lifetime distributions. Changes in the PSII Chl *a* fluorescence lifetime distributions can yield valuable information about the pigment–protein conformation and photochemical events in PSII (6,27,29,30). We have compared the effects of these two highly contrasting mechanisms under conditions of max-

imal fluorescence, where all photochemical fluorescence quenching by the primary electron acceptor of PSII (Q_A) is inhibited. This was done by including the herbicide 3-(3,4-dichlorophenyl)-1,1-dimethylurea (DCMU) that keeps all Q_A in the Q_A^- state. Earlier time-resolved studies (6,29) showed that under these conditions, the trans-thylakoid membrane proton gradient (ΔpH) and xanthophyll cycle caused separate and concerted changes in the Chl *a*-containing antennae protein conformation. It remained to be determined what types of changes in the PSII Chl *a* fluorescence lifetimes, when analyzed using a Lorentzian distribution model, are associated with the photoinhibitory mechanism, although it is well established that photoinhibition is independent of both the xanthophyll cycle and ΔpH (31–33). In this paper, we report that comparative measurements of these two contrasting PSII Chl *a* fluorescence quenching conditions revealed distinctively different effects both on the fluorescence lifetime distributions and on the relationships between the average fluorescence lifetime and steady-state intensity.

MATERIALS AND METHODS

Time-resolved PSII Chl *a* fluorescence measurements. The PSII Chl *a* fluorescence lifetimes were measured with a multifrequency cross-correlation fluorometer (model K2, ISS Instruments, Urbana, IL, USA). The average photon flux density (PFD) of the sinusoidally modulated sample excitation was $22 \pm 2 \mu\text{mol m}^{-2} \text{s}^{-1}$ at 610 nm and was provided by a cavity-dumped rhodamine 6G dye laser (Coherent, Palo Alto) pumped by a mode-locked Nd:YAG laser (Coherent, Palo Alto). Data were collected at 16 separate frequencies of the sinusoidally modulated excitation ranging from 7 to 300 MHz. The frequencies were mixed randomly during acquisition to minimize systematic errors from sample bleaching and heterogeneity. The sample emission was collected under "magic-angle" conditions with the excitation and emission monochromator polarizers set at 0° and 54.7° , respectively. Light scattering from a glycogen suspension was used for the 0 ns lifetime reference. The shift in phase angles (phase shift) and demodulation ratios (modulation) of the sample fluorescence emission were recorded and analyzed as described below. A complete explanation of the multifrequency cross-correlation technique, including the equations describing the phase shift and modulation, can be found in Govindjee *et al.* (27,30).

Plant material and thylakoid isolation. Seeds of wild-type barley (*Hordeum vulgare* L. cv. Donaria) were kindly provided by Dr. D. Simpson of the Carlsberg Research Laboratories, Copenhagen Valby, Denmark. Seeds were germinated on a heating pad in potting soil covered with a layer of vermiculite. Plants were watered twice daily and fertilized once with a 20 N:20 P:20 K fertilizer applied at a concentration of 473 ppm N. Plants were grown in a glasshouse with supplemental high-intensity discharge lamps; the minimum PFD was $400 \pm 100 \mu\text{mol photons m}^{-2} \text{s}^{-1}$ and the photoperiod was 14 h light and 10 h dark. Plants were harvested for thylakoid isolation after 8–10 days growth; they were dark adapted for at least 12 h at room temperature, then cut at their base, wrapped in a wet paper towel and chilled in the dark for 1–2 h in a bag of ice in a 4°C refrigerator. All thylakoid isolation procedures were performed in a darkened cold room (7°C) under dim green light using chilled wares. The leaves (8–10 g) were cut into 2–3 cm pieces and ground using 2–3 1 s bursts in a Waring blender in 100 mL of a slushy grinding buffer containing 0.33 M dextrose, 50 mM $\text{Na}_2\text{HPO}_4 \cdot 7\text{H}_2\text{O}$, 50 mM KH_2PO_4 , 25 mM KCl, 5 mM MgCl_2 , 0.1% bovine serum albumin (BSA), 0.2% Na-ascorbate, pH 6.5. The brie was gently vacuum filtered through 41 μm nylon filter (Spectra/Mesh). The filtrate was centrifuged for 10 min at 1500 *g* in an SS-34 (Sorvall) rotor at 4°C . The chloroplast pellet was gently resuspended in 0.5–1 mL of a buffer containing 0.33 M sorbitol, 4 mM EDTA, 5 mM MgCl_2 , 2 mM MnCl_2 , 0.1 M HEPES, 0.2% BSA, pH 7.6. The basic reaction mixture contained 0.1 M sucrose, 10 mM NaCl, 10 mM KCl, 5 mM MgCl_2 , 10 mM Tricine, 1 mM KH_2PO_4 , 0.2% BSA, pH 8.0. The following ingredients were added to the reaction mixture

immediately prior to the experiments: 30 mM Na-ascorbate to mediate V deepoxidation (17), 50 μM methylviologen to mediate linear electron transport and 0.3 mM ATP to fuel ATP hydrolysis. The Chl concentration was determined according to the equations of Graan and Ort (34); similar results (not shown) were obtained with the equations of Porra *et al.* (35).

Xanthophyll cycle-dependent nonphotochemical quenching of PSII Chl *a* fluorescence. Prior to actinic illumination, the chloroplast envelopes were osmotically ruptured by diluting the chloroplast suspension, obtained above, 10-fold in a 5 mM MgCl_2 solution (0.5–1.0 mL) for 15 s in a magnetically stirred, water-jacketed reaction cuvette (15°C). The thylakoid membranes, thus obtained, were brought to a final concentration of 15 μM Chl *a* + *b* in the reaction mixture described above.

To induce V deepoxidation, the thylakoid membrane suspension was illuminated for 15 min, from the top of the cuvette, through the fiber-optic probe of the pulse-amplitude modulation (PAM) 103 chlorophyll fluorometer (Heinz-Walz, Effeltrich, Germany) with a white light provided by a microscope lamp (Unitron), passed through a Corning CS1-75 infrared filter; the PFD measured at the surface of the reaction mixture was $500 \mu\text{mol m}^{-2} \text{s}^{-1}$. To vary the degree of V deepoxidation, dithiothreitol (36) was added at varying low concentrations, $0.25 < x < 1 \text{ mM}$, prior to the white light illumination. For conditions of high V deepoxidation dithiothreitol was omitted for the first 15 min of illumination; then, in all cases dithiothreitol (3 mM) was added for two purposes: (1) to inhibit any further V deepoxidation (36) and (2) to reduce the γ -subunits of the chloroplast coupling factor and activate ATPase activity (37,38). Also, in all cases, the white light illumination was continued for a total of 20 min at which point the sample was darkened. A 1.5 mL portion of this light-treated chloroplast suspension was frozen immediately in a microfuge tube by immersion in liquid nitrogen and stored at -80°C until the pigment content was analyzed by HPLC according to Gilmore and Yamamoto (39). Another 1.5 mL portion of the light-treated thylakoid suspension was removed and mixed in 1.5 mL of the same reaction mixture such that the final [Chl *a* + *b*] = 7.5 μM ; 10 μM DCMU was added to ensure reduction of the primary quinone electron acceptor of PSII, Q_A , and all other reagent concentrations remain unchanged (see Fig. 1 legend for details). This mixture, which was placed in the dark on ice for around 5 min, contained an activated ATPase, a ΔpH , and Z + A and consequently had a lowered or "quenched" yield of PSII Chl *a* fluorescence due to xanthophyll cycle-dependent nonphotochemical quenching.

The thylakoid sample under the quenched PSII Chl *a* fluorescence conditions was then transferred from the ice to a $1 \times 1 \text{ cm}$ quartz fluorescence cuvette and placed in the stirred sample compartment (2°C) of the multifrequency cross-correlation fluorometer apparatus described above; the temperature of the sample was allowed to equilibrate for 5 min prior to data acquisition. The multifrequency phase shift and modulation data for the quenched sample conditions were obtained as described earlier (6,29). After the lifetime measurements, the sample was immediately ($< 15 \text{ s}$) placed under the fiberoptic probe of the PAM fluorometer while the quenched PSII Chl *a* fluorescence intensity (F'_m) was measured with the pulsed measuring beam set at 100 kHz and with an additional strong white light (PFD = $500 \mu\text{mol m}^{-2} \text{s}^{-1}$). After measuring the F'_m fluorescence intensity for 10–15 s, 2 μM nigericin was added to the sample to uncouple the ΔpH and reverse all xanthophyll cycle-dependent nonphotochemical quenching of the PSII Chl *a* fluorescence. Following the addition of nigericin, the maximal fluorescence intensity (F_m) under the unquenched sample conditions was measured for at least 60 s. The level of xanthophyll cycle-dependent nonphotochemical quenching of the PSII Chl *a* fluorescence intensity was calculated as $(F_m/F'_m - 1)$. The multifrequency phase shift and modulation ratio data were then collected for the unquenched sample conditions as described above.

Photoinhibitory nonphotochemical quenching of PSII Chl *a* fluorescence. The sample preparation for photoinhibitory quenching was exactly as described above for the xanthophyll cycle-dependent nonphotochemical quenching conditions except that all samples were treated with 3 mM dithiothreitol prior to the 20 min PFD = $500 \mu\text{mol m}^{-2} \text{s}^{-1}$, white light illumination. After this white light illumination, the samples were diluted with reaction mixture such that all other ingredients remained the same, the final Chl *a* + *b*

concentration was $7.5 \mu\text{M}$, and DCMU was $10 \mu\text{M}$. The samples were then treated with $2 \mu\text{M}$ nigericin to uncouple the ΔpH and, thus, ensure that there was no xanthophyll cycle-dependent nonphotochemical quenching of the PSII Chl *a* fluorescence. The PSII Chl *a* fluorescence lifetime (phase shift and modulation) data were acquired for these samples as described above. The samples were transferred back to the 15°C cuvette used for the white light illumination above. The PSII Chl *a* fluorescence intensity was continuously monitored with the PAM measuring beam set at 100 kHz and starting from the maximal intensity F_m as the photoinhibitory light treatment was administered for periods ranging from 5 to 90 min. The high-intensity white light used for the photoinhibitory treatment was provided by a Schott model K1500 lamp passed through a Walz DT-Cyan infrared filter and the PAM fiberoptic probe; the PFD measured at the surface of the samples was $4500 \mu\text{mol m}^{-2} \text{s}^{-1}$. At the end of each photoinhibitory light treatment, the final PSII Chl *a* fluorescence intensity (F_m) was determined. The level of the photoinhibitory nonphotochemical quenching of PSII Chl *a* fluorescence was calculated as $(F_m/F_{m_i} - 1)$. The samples were placed back into a $1 \times 1 \text{ cm}$ quartz fluorescence cuvette and the multifrequency phase shift and modulation data were obtained, as described above.

Analysis of multifrequency cross-correlation phase shift and modulation data. The acquired multifrequency phase shift and modulation data were fit to fluorescence lifetimes with either a bimodal Lorentzian distribution model or a multicomponent discrete exponential model using Globals Unlimited© software (Laboratory for Fluorescence Dynamics, Physics Department, University of Illinois at Urbana-Champaign, Urbana, IL). The fluorescence lifetime data were analyzed and presented as the lifetime centers (τ_c) and their respective fractional intensities (f_c). The χ^2 values for the fits did not improve by inclusion of more than the reported number of Lorentzian distributions or discrete exponential components; inclusion of another lifetime component either resulted in a duplicate lifetime value and/or in components with physically suspect values.

RESULTS

Comparison of the effects of photoinhibition and xanthophyll cycle-dependent changes on the PSII Chl *a* fluorescence lifetimes and intensity

Figure 2 shows representative multifrequency phase shift (open symbols) and modulation (cross-filled symbols) data obtained with barley thylakoids subjected to conditions of relatively high and low levels of either (A) xanthophyll cycle-dependent or (B) photoinhibition nonphotochemical quenching of the PSII Chl *a* fluorescence. The high (squares) and low (circles) levels of the xanthophyll cycle-dependent fluorescence quenching conditions in Fig. 2A were obtained with barley thylakoids in the presence of an ATPase-mediated ΔpH and high and low $Z + A$ concentrations, 35.8 and $7.4 \text{ mmol } Z + A (\text{mol Chl } a + b)^{-1}$, respectively. Clearly, the sample with the high $Z + A$ concentration, $[Z + A]$, had lower phase shift values and higher modulation, especially at the higher frequencies; this indicated a lower average PSII Chl *a* fluorescence lifetime in the high $[Z + A]$ sample. The phase shift and modulation data in Fig. 2C were measured using the same high and low $[Z + A]$ barley thylakoid samples from Fig. 2A after treatment of the samples with nigericin to uncouple the ΔpH and eliminate the xanthophyll cycle-dependent nonphotochemical fluorescence quenching. Uncoupling the ΔpH with nigericin increased the phase shift and decreased the modulation resulting in the same final levels for both samples. It was clear that the $[Z + A]$ did not affect the PSII Chl *a* fluorescence phase and modulation without a ΔpH . The high and low levels of the photoinhi-

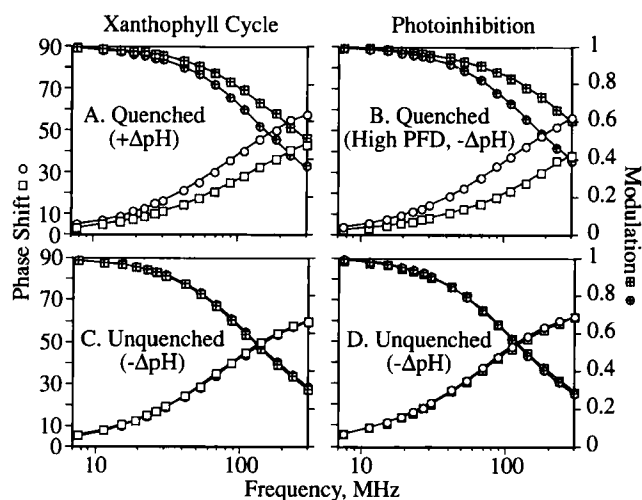


Figure 2. The multifrequency phase shift (open symbols) and modulation (cross filled symbols) values describing the PSII Chl *a* fluorescence in barley thylakoids under conditions relating to either xanthophyll cycle-dependent (A,C) or photoinhibitory (B,D) quenching. A shows effects of high and low $Z + A$ concentration (squares $[Z + A] = 35.8$, circles $[Z + A] = 7.4 \text{ mmol } Z + A \text{ mol}^{-1} \text{ Chl } a + b$) in barley thylakoids with a ΔpH . C shows the effects of uncoupling the ΔpH in the barley thylakoid samples in A; the levels of the $Z + A$ remain unchanged between A and C. B shows the effects of exposure to a high PFD for 90 min (squares) and 5 min (circles) of barley thylakoids with an uncoupled ΔpH and only low $[Z + A]$ ($\approx 7 \text{ mmol } Z + A [\text{mol Chl } a + b]^{-1}$). D shows the same barley thylakoid samples and conditions as in B before any exposure to the high PFD. The phase shift = $\tan^{-1}(S[\lambda, \omega]/G[\lambda, \omega])$ and modulation = $(S^2[\lambda, \omega] + G^2[\lambda, \omega])^{1/2}$, where $S(\lambda, \omega)$ and $G(\lambda, \omega)$ are the normalized sine and cosine Fourier transforms of the fluorescence intensity $I(\lambda, t)$, see Govindjee *et al.* (22,32). In addition to the variable levels of $[Z + A]$ mentioned above, the unquenched (3 mL) thylakoid reaction mixtures in C and D contained $7.5 \mu\text{M}$ Chl *a* + *b*, $10 \mu\text{M}$ DCMU, $2 \mu\text{M}$ nigericin, 30 mM Na-ascorbate, $50 \mu\text{M}$ methylviologen, 0.3 mM ATP, 0.1 M sucrose, 10 mM NaCl, 10 mM KCl, 5 mM MgCl_2 , 10 mM Tricine, 1 mM KH_2PO_4 , 0.2% BSA, pH 8.0. The quenched sample reaction mixtures in A were the same as in C except without nigericin; the quenched sample reaction mixtures in B were the same as in D.

bitory nonphotochemical fluorescence quenching in Fig. 2B were obtained with barley thylakoids treated for a long time (90 min, squares) or a short time (5 min, circles), respectively, with the high PFD ($4500 \mu\text{mol photons m}^{-2} \text{s}^{-1}$) at 15°C in the absence of a ΔpH and with only low levels of $Z + A$. In the sample treated for 90 min, the phase shift was lower and the modulation was higher than in the 5 min sample, indicating a clearly lowered average PSII Chl *a* fluorescence lifetime in the 90 min sample. The phase shift and modulation data in Fig. 2D simply show the control photoinhibition data measured prior to the high (90 min) and low (5 min) thylakoid samples shown in Fig. 2B. It is clear in Fig. 2D that both samples started out with similar phase shift and modulation prior to the photoinhibitory treatments.

Table 1 shows a comparison of the mean \pm SE values for the χ^2 values of the phase shift and modulation ratio data fit to either a bimodal Lorentzian distribution analysis (Lorentzian) or a three-component exponential analysis (exponential) for the PSII Chl *a* fluorescence lifetimes. The data represent all the (n) analyzed samples under the quenched and unquenched conditions for both the xanthophyll cycle-dependent and photoinhibition quenching mechanisms. Over-

Table 1. The reduced χ^2 values for the fits of the multifrequency phase and modulation data to both bimodal Lorentzian distribution analysis (Lorentzian) and three-component exponential analysis (exponential) for barley thylakoids

	Xanthophyll cycle* (n = 19)		Photoinhibition† (n = 7)	
	Unquenched	Quenched	Unquenched	Quenched
χ^2 (Lorentzian)	1.53 ± 0.32	2.36 ± 0.21	0.66 ± 0.07	1.31 ± 0.27
χ^2 (exponential)	1.67 ± 0.29	2.42 ± 0.20	1.06 ± 0.12	1.39 ± 0.24

*Unquenched sample conditions were defined in Fig. 1C (no Δ pH and varying levels of [Z + A]). Quenched sample conditions were defined in Fig. 1A (an ATPase-mediated Δ pH and varying levels of [Z + A]).

†Unquenched sample conditions were defined in Fig. 1D (no Δ pH, low [Z + A] and no exposure to excessive PFD). Quenched sample conditions were defined in Fig. 1B (no Δ pH, low [Z + A] and varying times of exposure to excessive PFD).

all, the quality of the fits was roughly equivalent for both mechanisms. The residuals were randomly distributed around the mean in all cases with little or no indication of a systematic error with respect to frequency. In contrast to the unquenched sample conditions, the χ^2 values were slightly larger in the quenched sample conditions because of a lower overall signal-to-noise ratio.

The bimodal Lorentzian model resulted in slightly better fits (lower χ^2 values) on average for all conditions and both quenching mechanisms when compared to the three-component exponential decay model. Therefore, our explanation of the relationship between the PSII Chl *a* fluorescence intensity and the fluorescence lifetime components is primarily based on the Lorentzian distribution model. Further, the following analysis of the time-resolved data using the Lorentzian distribution model accepts the following three physical assumptions: (1) that the lifetime of the excited state of Chl is strongly influenced by its physical environment, (2) that the various pigment-protein complexes that contain (bind) Chl, like other proteins studied (40), exist in a distribution of multiple conformational substates or shapes and (3) that the different conformational substates may interconvert within the time scale of the Chl* excited state lifetime (27,30).

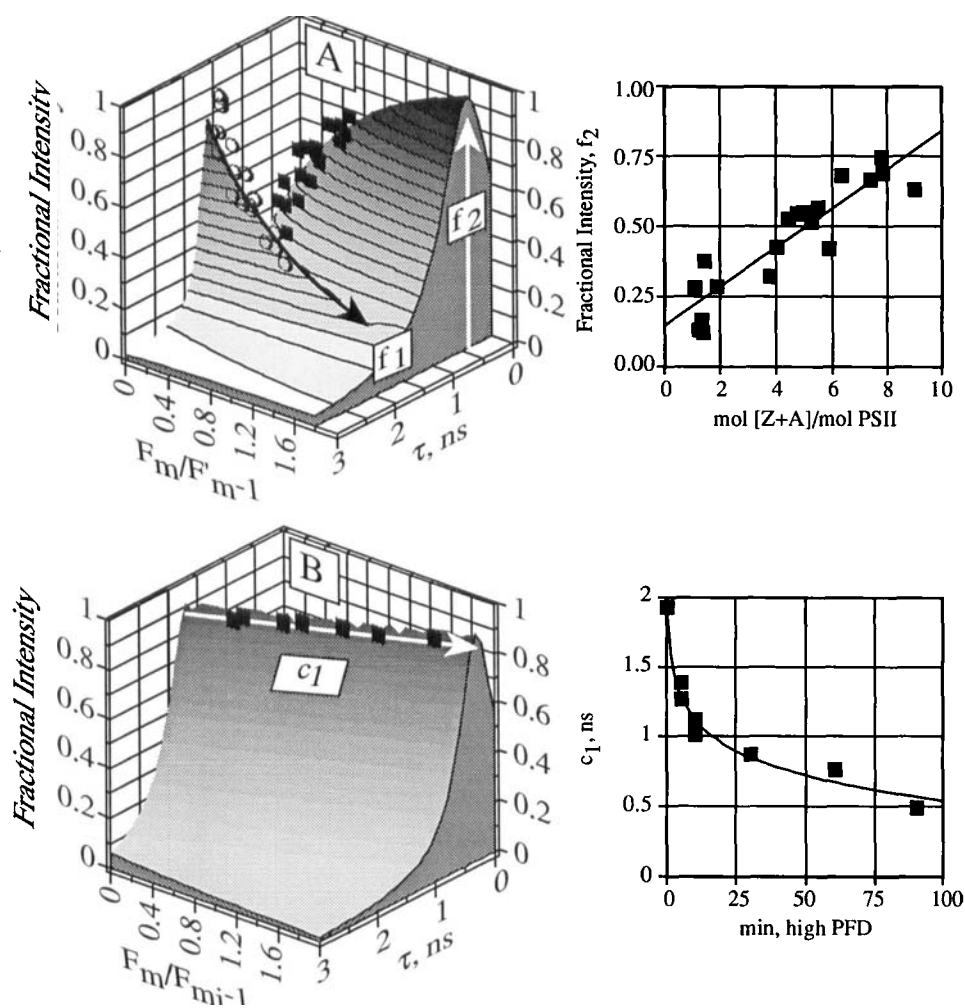
Figure 3 compares, using three-dimensional surface plots, the PSII Chl *a* fluorescence lifetime distributions under conditions of varying levels of xanthophyll cycle-dependent (A) or photoinhibition-dependent (B) nonphotochemical quenching of PSII Chl *a* fluorescence. In the absence of either xanthophyll cycle-dependent or photoinhibitory nonphotochemical quenching on the PSII Chl *a* fluorescence lifetime distributions (not shown) were homogeneous, being distinguished by a main lifetime distribution center $c_1 \approx 1.9$ ns, a fractional intensity $f_1 \geq 93\%$ and a width $w_1 \approx 0.8$ ns; the much narrower minor ($f_2 \leq 7\%$) lifetime distribution (c_2) was centered in the 20–200 ps range, see Gilmore *et al.* (29). These conditions corresponded to the maximal PSII Chl *a* fluorescence yield, F_m , described in the Materials and Methods.

Figure 3A illustrates the effects that the ATPase-mediated Δ pH and xanthophyll cycle deepoxidation exert on the fluorescence lifetime distributions. The sample conditions corresponded to a quenched or decreased yield for the PSII Chl *a* fluorescence intensity (F'_m) as described in the Materials and Methods. The surface of the three-dimensional plot in Fig. 3A was plotted using the average width and lifetime center values for both the Lorentzian distributions with the

Δ pH (see Fig. 3 legend). The symbols show the relationship between the average lifetime center values ($c_1 = 1.6$ ns, $c_2 = 0.4$ ns) and the actual f_1 and f_2 fractional intensity values (circles and squares, respectively) and ($F_m/F'_m - 1$) values. Both, the lifetime center and width values of the longer lifetime distribution decrease to $c_1 \approx 1.6$ ns and $w_1 \approx 0.3$ ns from those without a Δ pH, namely, $c_1 \approx 1.9$ ns and $w_1 \approx 0.75$ ns. Importantly, however, the lifetime centers of the two distributions (Fig. 3A) remained constant independent of the fluorescence intensity ($F_m/F'_m - 1$). What is also clear in Fig. 3A is that as the PSII Chl *a* fluorescence intensity is decreased (with increasing values for $F_m/F'_m - 1$) the fractional intensity of the 0.4 ns distribution (f_2 , white arrow) increases at the expense of f_1 (dark arrow). As described by Gilmore *et al.* (29) the predicted curvilinear function was used to plot the surface of the three-dimensional plot that describes the relationship between the f_1 and f_2 fractional intensities and ($F_m/F'_m - 1$). The inset next to Fig. 3A shows that the f_2 fractional intensity correlates with increasing concentrations of Z + A; these data are from the same samples and conditions as shown in Fig. 3A. These results confirm and extend those reported earlier with barley wild-type thylakoids in Gilmore *et al.* (29).

Figure 3B shows the effects of varying times of exposure to the highly excessive photoinhibitory PFD on the PSII Chl *a* fluorescence lifetime distributions in barley thylakoids. The experimental conditions further included the absence of a Δ pH and only low levels of Z + A (see Fig. 3 legend) in the barley thylakoid samples. It is stressed that although these conditions are physiologically harsh and unnatural, that they are, in comparison, very consistent with similar experimental conditions routinely used in the current literature to study photoinhibition (8–13). These sample conditions corresponded to a decreased yield of PSII Chl *a* fluorescence (F_{mi}) as described in the Materials and Methods. Figure 3B shows that the photoinhibitory treatments progressively decrease the lifetime center value c_1 (white arrow); all the other Lorentzian distribution parameters remained within the given standard error ranges listed in the Fig. 3 legend. The inset next to Fig. 3B shows the slow kinetics of the decreases in the fluorescence lifetime center c_1 during exposure to the high photoinhibitory PFD. The surface of Fig. 3B was plotted using the average fractional intensity and width values for all the photoinhibition samples; the relationship between the lifetime center c_1 and ($F_m/F_{mi} - 1$) fit well to the linear equation ($[F_m/F_{mi} - 1] = [c_1 \times -0.695] + 1.68$; $n = 7$; $r^2 = 0.98$), which was used to plot the c_1 lifetime center values

Figure 3. Relationship between the PSII Chl *a* fluorescence intensity and the bimodal Lorentzian fluorescence lifetime distributions in barley thylakoids under conditions of (A) varying levels of xanthophyll cycle-dependent energy dissipation and (B) varying levels of photoinhibition energy dissipation. The conditions for A included the presence of an ATPase-mediated ΔpH and varying levels of [Z + A]. The surface of Fig. 3A was plotted using the average lifetime centers ($c_1 = 1.61 \pm 0.02$ ns, $c_2 = 0.40 \pm 0.03$ ns) and widths ($w_1 = 0.30 \pm 0.02$ ns, $w_2 = 1.06 \pm 0.06$ ns) for all thylakoid samples under these conditions. The modeled changes in the fractional intensity values shown in the surface plot A were obtained as described by Gilmore *et al.* (29) by substituting the following equality for $F'_m = -0.839(f_2) + 1.196$ ($r^2 = 0.897$) for varying levels of $(F_m/F'_m - 1)$, where F_m was normalized to 1 and f_2 is the fractional intensity of the 0.4 ns distribution (see arrow); the sample size was $n = 19$ (squares for f_2 and open circles for f_1). The inset to the right of Fig. 3A shows the linear relationship between the number of Z + A molecules per PSII (on a total Chl *a* + *b* basis estimated as described by Gilmore *et al.* (29)) and the fractional intensity of f_2 under the same conditions and in the same thylakoid samples as in Fig. 3A. The conditions for B included the absence of a ΔpH , low, ≈ 7 mmol Z + A (mol Chl *a* + *b*) $^{-1}$, and varying times of exposure to the high, excessive PFD; the inset next to Fig. 3B shows the kinetics of the decrease in the lifetime center value of c_1 during exposure to the high PFD. The surface of Fig. 3B was plotted using the average fractional intensity ($f_1 = 0.92 \pm 0.00$, $f_2 = 0.08 \pm 0.01$) and width ($w_1 = 0.72 \pm 0.02$ ns, $w_2 = 0.01 \pm 0.00$ ns) parameters for all the thylakoid samples under these conditions.



for the surface plot. The solid square symbols show that the decreases in the lifetime center (c_1), correlated highly with the decreased fluorescence intensity ($F_m/F_{mi} - 1$) measured in parallel.

In Table 2 we show data from barley thylakoid samples before, after 5 min and after 90 min of the photoinhibitory

high-PFD treatment. These data were fit to the three-component exponential decay model. The data in Table 2 show that with increasing time of exposure to the photoinhibitory PFD, the largest change is the decrease in the lifetime center of the main ≈ 2 ns component (c_2) that itself is likely attributable to the PSII charge separation process (9,27,41); thus,

Table 2. Effects of increasing times of exposure to excessive photon flux density (photoinhibition) on the lifetime centers ($c_x = \text{ns}$) and fractional intensities (f_x) for a three-component exponential fluorescence decay model in barley thylakoids; also shown are the calculated average PSII Chl *a* fluorescence lifetimes $\langle\tau\rangle$ and $\langle\tau\rangle'$ and the reduced χ^2 values for the fits*

Exposure	c_1 (f_1)	c_2 (f_2)	c_3 (f_3)		χ^2
0 min	5.80 (0.116)	1.87 (0.753)	0.37 (0.131)	$\langle\tau\rangle = 2.129$	1.336
5 min	6.66 (0.066)	1.49 (0.717)	0.35 (0.217)	$\langle\tau\rangle' = 1.584$	0.603
90 min	4.23 (0.104)	0.75 (0.603)	0.16 (0.293)	$\langle\tau\rangle' = 0.939$	2.206

* $\langle\tau\rangle$ or $\langle\tau\rangle' = \sum c_x f_x$ for each exposure condition.

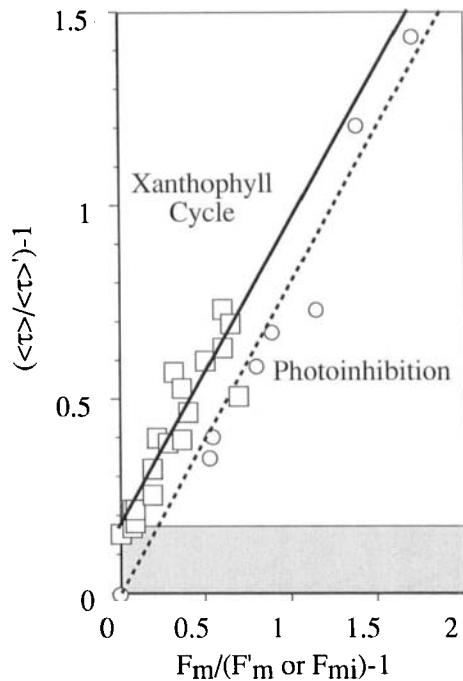


Figure 4. The linear relationship between the changes in the average fluorescence lifetimes measured as $(\langle\tau\rangle/\langle\tau\rangle' - 1)$ and the decreases in the average lifetime of PSII Chl *a* fluorescence as affected by the xanthophyll cycle (squares) and photoinhibition (circles) non-photochemical quenching mechanisms. The linear regression statistics of the fits are shown in Table 2. The height of the gray box at the bottom of Fig. 4 represents the value of the y-intercept for the xanthophyll cycle plot. See list of abbreviations for definition of symbols used.

the decreases in the average lifetime from $\langle\tau\rangle$ in the unquenched time = 0 sample to $\langle\tau\rangle'$ in the 5 and 90 min-treated samples are explained mostly by the decrease in c_2 . However, in the 90 min sample there are also clear decreases in both c_1 and c_3 components. Although the physical origin of the slow c_1 lifetime component is questionable and possibly attributable to "free Chl," the fast c_3 component is most likely attributable to PSI and the fast exciton equilibration processes throughout the antennae Chl (27,41). In any case, the patterns of these decreases were significant because it is known that quenching of PSII Chl *a* fluorescence due to the accumulation of doubly reduced Q_A , Q_A^{2-} , in the PSII reaction center is distinguishable by the formation of a long (≈ 10 ns) component (12,27,28). No such long-lifetime component was observed in our photoinhibition samples using either the Lorentzian (Fig. 3) or multiexponential analysis (Table 2).

Different effects of xanthophyll cycle-dependent and photoinhibition nonphotochemical quenching mechanisms on the relationship between the decreased intensity and average lifetimes of PSII Chl *a* fluorescence

In Fig. 4 we compare the effects of the xanthophyll cycle-dependent (square) and photoinhibitory (circles) PSII Chl *a* fluorescence quenching mechanisms with respect to the relationship between the decrease in the average fluorescence lifetime and the decrease in the fluorescence intensity. We calculated the average lifetimes and measured the intensity

Table 3. Linear regression statistics* for the plots of xanthophyll cycle-dependent and photoinhibition-dependent of quenching the PSII Chl *a* fluorescence, $F_m/(F'_m \text{ or } F_{mi}) - 1$, against the decrease in the average PSII Chl *a* fluorescence lifetime, $\langle\tau\rangle/\langle\tau\rangle' - 1$, shown in Fig. 4

Model Equation: $(\langle\tau\rangle/\langle\tau\rangle' - 1) = \text{slope} (F_m/[F'_m \text{ or } F_{mi}] - 1) + \text{intercept}$		
	Xanthophyll cycle	Photoinhibition
n	19	14†
Slope (<i>P</i>)	0.79 ± 0.08 (1.28×10^{-8})	0.81 ± 0.03 (1.52×10^{-12})
Intercept (<i>P</i>)	0.17 ± 0.03 (2.36×10^{-5})	-0.02 ± 0.02 ($\ddagger 0.51$)
r^2	0.85 ± 0.08	0.98 ± 0.07

* r^2 , coefficient of determination; *P*, probability for null hypothesis of the slope or intercept parameter. The values given are the mean \pm SE.

†Sample size includes the zero time sample measurements for all seven samples that were treated under the photoinhibitory conditions for more than 5 min.

‡This *P*-value can be disregarded for the reasons explained in the text.

for each sample in the presence of the xanthophyll cycle-dependent and photoinhibition nonphotochemical quenching ($\langle\tau\rangle'$ and F'_m and F_{mi}) and in their absence ($\langle\tau\rangle$ and F_m) as described in the Materials and Methods. The average lifetimes $\langle\tau\rangle$ and $\langle\tau\rangle'$ were calculated from a three-component exponential fluorescence decay model for the PSII Chl *a* fluorescence as described in Table 2 above. In Table 3 we provide the linear regression statistics of the data fits shown in Fig. 4. First, it is clear from the values of the coefficients of determination (r^2) that both mechanisms show significant linear relationships between the decreasing PSII Chl *a* fluorescence intensity ($F_m/[F'_m \text{ or } F_{mi}] - 1$) and the decreasing average lifetime calculated as $(\langle\tau\rangle/\langle\tau\rangle' - 1)$. More importantly, however, Fig. 4 and Table 3 both show that the y-intercept values for the intensity vs the average lifetime plots of these two different fluorescence quenching mechanisms are significantly different. For the xanthophyll cycle-dependent quenching mechanism (Fig. 4, squares) there is a clear and statistically significant (low *P*-value) y-intercept of 0.17 ± 0.03 . The photoinhibition mechanism shows an intercept standard error range virtually at or below the origin. This intercept (-0.02 ± 0.02) has a very low standard error but has a high *P*-value; the high *P*-value can be disregarded and is attributable only to the relative uncertainty of an intercept that has a very small absolute value because it is very close to the origin. In this case, the statistics in Table 3 indicate that there was certainly no overlap within the SE ranges of the y-intercept values between the photoinhibitory and xanthophyll cycle-dependent quenching mechanisms.

DISCUSSION

The novelty of results in this paper lies in showing that the xanthophyll cycle- and photoinhibition-dependent mechanisms are distinguishable by their differing effects on the PSII Chl *a* fluorescence lifetimes and steady-state fluorescence intensity. We discuss these effects with respect to our current basic model of PSII exciton dynamics, structure and

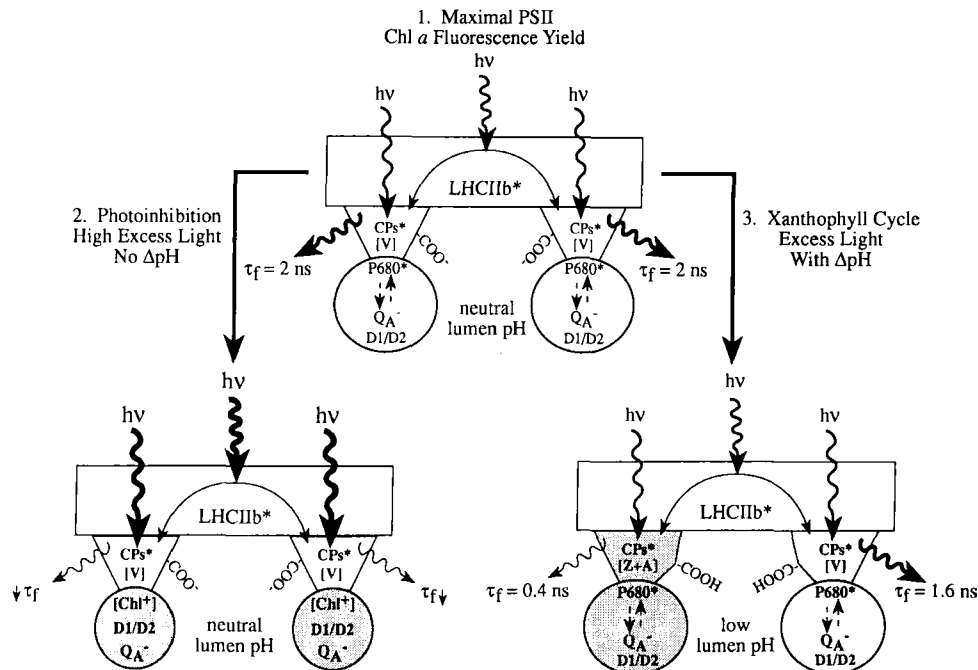


Figure 5. A schematic comparison of the xanthophyll cycle and photoinhibition nonphotochemical mechanisms on maximal yields of PSII Chl *a* fluorescence. The role of the peripheral PSII antenna, LHCIIb, is described in the text. Absorbed light energy ($h\nu$) leads to the excited state of the peripheral antenna (LHCIIb*) and the inner antenna (CP*). The CPs are shown to be enriched with the xanthophyll cycle pigments [V] and [Z + A]. The absorbed light energy from the antennae causes the formation of the singlet excited P680 (P680*) special pair Chl in the core PSII reaction center D1/D2 complex; the D1/D2 complex is shown to contain the reduced primary quinone electron acceptor, Q_A^- , as in our experimental conditions. Condition 1 (top) describes the maximal PSII Chl *a* fluorescence conditions that exist in the absence of either the xanthophyll cycle or photoinhibition effects. Maximal PSII fluorescence conditions are also shown here as having a high ratio of V to Z + A = [V] as well as unprotonated CP proteins ($-\text{COO}^-$). Condition 2 (left) shows the effects of exposure to high PFD that lead to photoinhibitory damage in the absence of a ΔpH and independent of V deepoxidation. Here, it is proposed that increased concentrations of oxidized Chl species, such as Chl cations or $[\text{Chl}^+]$, are the most likely quenchers of the Chl *a* fluorescence. The decreased size of the core PSII reaction center D1/D2 compartment symbolizes the high light-induced degradation of PSII. The thickness of the τ_f arrows and the shading of the core PSII unit symbolize the increased heat dissipation in the PSII core and decrease in τ_f when compared to condition 1. Photoinhibition effects are proposed to be relatively homogeneous for all PSII units. Condition 3 (right) shows the complex effects associated with the ΔpH (low-lumen pH) and the xanthophyll cycle nonphotochemical quenching mechanism. Here the CP proteins are shown to be protonated (COOH) and the overall conformation of the inner antennae is shown to be different than under condition 1. The PSII units with a higher [Z + A] are shaded and have shorter τ_f values than those with high [V]. As under condition 2, the thickness of the τ_f arrows and the shading of the PSII unit symbolize the increased heat dissipation and decreased τ_f .

function as presented in Gilmore *et al.* (29). According to that study of the PSII Chl *a* fluorescence lifetimes and intensity, the presence or concentration of LHCIIb does not affect the PSII Chl *a* fluorescence lifetimes, the quantum yield of PSII photochemistry or the xanthophyll cycle-dependent nonphotochemical quenching mechanism. We note that these conclusions contradict earlier held theories that the exciton lifetime should be directly related to the PSII Chl *a* + *b* antenna size or N_{pig} (41–43). However, Gilmore *et al.* (29) presented the first direct comparison of the effects of N_{pig} on the PSII Chl *a* fluorescence lifetimes in both native (nondetergent-treated) thylakoid membranes and leaves; moreover, both the *in vivo* levels of PSII photochemical efficiency and xanthophyll cycle-dependent nonphotochemical quenching (NPQ) were preserved. Thus, we conclude that discrepancies between the Gilmore *et al.* (29) data and ideas and those of other researchers working with detergent-treated subchloroplast particles and membranes (44,45) may be attributable to the effects of detergent on the delicate *in vivo* energy transfer processes of PSII. Further, our data confirm and extend the results and conclusions obtained independently by Briantais *et al.* (46) as well as by Lin and Knox

(47) that showed the main light-harvesting pigment–protein complex of PSII (LHCIIb)-dependent fluorescence component is very short-lived ($\ll 100$ ps) and therefore does not make a substantial contribution to the PSII average fluorescence lifetime or steady-state intensity at room temperature. Figure 5 summarizes some of the current concepts; here, we depict LHCIIb as having a primarily light-harvesting role and a negligible quantum yield for fluorescence due to a rapid and efficient transfer of absorbed energy to the PSII inner antenna (CP) and reaction center core (D1/D2) complex.

According to our interpretations of the PSII Chl *a* fluorescence lifetimes and intensity, condition 1 at the top of Fig. 5 represents the maximal *in vivo* PSII Chl *a* fluorescence quantum yield. Maximal fluorescence conditions minimally include the absence of a trans-thylakoid ΔpH (neutral lumen pH) and the presence of the reduced primary quinone electron acceptor of PSII, Q_A^- , as well as an intact reaction center. In our experiments, we met all three of the necessary conditions for maximal PSII Chl *a* fluorescence by utilizing the uncoupler nigericin to inhibit the ΔpH , adding DCMU to prevent oxidation of Q_A^- , use of healthy thylakoids (start-

ing with PSII quantum efficiency, F_v/F_m , values of 0.789 ± 0.001), as well as avoidance of exposure of the thylakoids to excess light for extended periods. Here we depict the maximal PSII Chl *a* fluorescence yield as a condition where the unprotonated PSII units (CP—D1/D2) have a similar main fluorescence lifetime distribution ($f = 0.9$) centered around 2 ns with a steady width around 0.8 ns. A relatively homogeneous conformation of the unprotonated PSII units is proposed to explain the main single fluorescence lifetime distribution under the maximal fluorescence conditions.

Condition 2 of Fig. 5 shows that exposure to excess light for extended periods, under the same conditions that would yield maximal PSII Chl *a* fluorescence, causes what we have defined here as aerobic photoinhibitory damage. As shown in the Results section, with increasing time of exposure to excess light there is a progressive decrease in the lifetime center of the main PSII Chl *a* fluorescence lifetime distribution (c_1), denoted here as τ_f . The photoinhibitory conditions in this study are quite similar in terms of atmospheric oxygen concentration, PFD and duration of light exposure to those used in similar studies where the patterns of P680 and D1 degradation were well documented (8,10,11). Therefore, we envision that the most likely cause of the gradual decrease in τ_f is symptomatic with the gradual oxidative degradation of the component pigment-proteins of PSII (mainly D1), as well as degradation and loss of the special P680 Chl of the PSII reaction center. Our time-resolved aerobic photoinhibition data and conclusions (see Table 2, Fig. 3) were also, in fact, quite similar to those of Renger *et al.* (9) who also showed a substantial decrease in the lifetime of all the fluorescence lifetime components, including the main 2 ns component that is associated with the charge-separation process (9,27,41), in response to increased exposure to excess PFD.

We did not see the pattern of fluorescence and lifetime changes that distinguish the presence of doubly reduced Q_A , namely, the formation of a very long lifetime component (≈ 10 ns) that itself has been attributed to the slow spin dephasing and recombination of the triplet radical pair to 3P680 (12,27,28). Therefore, we conclude that the fluorescence quenching under these photoinhibitory conditions is not due to an accumulation of Q_A^{2-} . Vass *et al.* (12) concluded independently that Q_A^{2-} does not accumulate under aerobic conditions similar to those in this study. Overall, our photoinhibition results are consistent with a gradual increase in the rate constant of a nonradiative decay pathway from the charge-separated state of the PSII reaction center; perhaps, the fluorescence quencher is related to the concentration and or redox potential of an oxidizing species such as a Chl⁺ cation and or the P680⁺ cation as suggested by others (9,13,24,25). We conclude that the photoinhibition effects are relatively homogenous for all the PSII units.

Condition 3 of Fig. 5 shows the sequential, switchlike changes that are associated with the xanthophyll cycle-dependent nonphotochemical quenching conditions. As explained in the introduction, the xanthophyll cycle mechanism is stimulated under excess light conditions that cause a trans-thylakoid Δ pH and thus acidify the chloroplast lumen; the chloroplast lumen acidification is a necessary precondition both for V deepoxidation to Z + A (17) as well as protonation of carboxyl groups (COO^-) of the CP proteins at the

luminal surface of the thylakoid membrane (5,19–21). It is suggested that the protonation of the carboxyl groups of the CP proteins causes a conformational switch or change in the Chl *a*-containing antennae proteins; this switch decreases the fluorescence lifetime center (τ_f) and width (w) of the longer distribution when compared to unprotonated (maximal fluorescence) condition 1 shown at the top of Fig. 5. This Δ pH-dependent shift is independent of the [Z + A] and is probably also associated with the positive y-intercept in the plot of the average lifetime *versus* the intensity as described in the Results (Fig. 4). The clear, positive y-axis intercept in the xanthophyll cycle-dependent plot for barley thylakoids in Fig. 4 was consistent with our previous report with spinach and lettuce thylakoids (6). We suggest the constant y-intercept change is due to the Δ pH-dependent conformational changes in the Chl *a*-containing PSII antennae proteins; such conformational changes should have been a constant factor in our experiments because of the constant ATPase-mediated Δ pH. We tentatively attribute the difference between the fluorescence intensity ($F_m/F'_m - 1$) and the average PSII Chl *a* fluorescence lifetime ($\langle \tau \rangle / \langle \tau \rangle' - 1$) during the xanthophyll cycle-dependent quenching (Fig. 4) to a change in the effective absorption cross section of the thylakoid samples associated with the pH-dependent conformational changes in the Chl *a*-containing antennae complexes. The changes in the c_1 component probably represent the low-lumen pH activation of the binding sites for Z + A in the inner antenna and the increases in the f_2 fractional intensity represent the concentration-dependent binding of Z + A. In contrast to the changes in the width and lifetime center of the c_1 component, it is clear that the f_2 (and f_1) fractional intensities are directly proportional to the [Z + A] (Fig. 3). Thus, we hypothesize that together these changes reflect the molecular sequence of events that cause xanthophyll cycle-dependent nonphotochemical quenching. We propose that the site of action of the xanthophylls is in the inner antenna complexes of PSII because the *chlorina* f104 barley mutant, which is highly deficient in the Chl *b*-containing LHCIIB retains near wild-type levels of the minor CP proteins of the PSII inner antenna (48) as well as wild-type levels of [Z + A]-dependent quenching (29).

Consistent with the model based on the above time-resolved data on barley thylakoids, a similar two-stage model was earlier proposed by Gilmore and Yamamoto (49) in the general form of the following model linear equation that yielded the best statistical fit to variations in xanthophyll cycle-dependent nonphotochemical quenching in isolated pea and lettuce thylakoids:

$$F_m/F'_m - 1 = x_1[Z + A][H^+] + x_2[H^+] + \text{constant}$$

where the x_1 term describes the [Z + A] concentration-dependent variable component at a given lumen proton concentration, $[H^+]$, and the x_2 term describes a [Z + A]-independent but lumen $[H^+]$ -dependent variable. Thus, we point out here the obvious respective analogies between x_1 term in the linear equation above and the [Z + A]-dependent changes in the f_2 component (Fig. 3) and the x_2 term and the Δ pH-dependent changes in the c_1 component (also in Fig. 3). We conclude that the two-stage models proposed by Gilmore *et al.* (29) and Gilmore and Yamamoto (49) and in this paper may account for the majority of "zeaxanthin-indepen-

dent" but Δ pH-dependent PSII Chl *a* fluorescence quenching in both leaves and chloroplasts (50–52). Indeed, these models predict high levels of fluorescence quenching with low levels of deepoxidized xanthophylls and high lumen $[H^+]$. First, it is important to consider that there are always background levels of $[Z + A]$ of around 1 to 2 mol $Z + A$ per PSII unit (based on a total Chl *a + b* basis) in fully dark-adapted barley, pea, lettuce and spinach leaf and chloroplast materials (6,29,49,53); it is also important to consider that even after high levels of deepoxidation in isolated chloroplasts there are normally fewer than 10 mol of $Z + A$ per PSII. Further, it is well known that significant levels of $Z + A$ exist in both the chloroplast envelope (54,55) and stromal lamellae (56–58). In sum, it is clear that the net maximal levels of $Z + A$ molecules per absolute PSII unit could be significantly less than 10. Nevertheless, if one assumes that a majority (even 50%) of the dark background levels $Z + A$ are functionally associated with PSII in the granal thylakoids, then it is clear that given both a high enough lumen $[H^+]$ and binding constant for the xanthophylls (relative to the protonated CP) that a majority of the PSII units could switch to the "quenched" conformation, without need for further deepoxidation. Thus, the stoichiometry of $[Z + A]$, relative to the absolute PSII unit, points to the likelihood that the xanthophylls act in a switch-like manner; this is inasmuch as their relatively low concentrations probably exclude them from exerting any gradual type of change at the level of inter- or intra-protein organization and conformation. With respect to the so-called xanthophyll cycle-independent fluorescence quenching, the Δ pH effects on the (c_1) fluorescence lifetimes of the "unquenched" PSII units may be considerable (perhaps more than 20–30 %) and quite variable between different plant species; indeed, the absolute lifetime values were significantly different for each plant species examined so far, including lettuce and spinach (6) and barley (29). Further, we conclude that the Δ pH-dependent ($[Z + A]$ -independent) changes to c_1 cannot be attributed to DCMU- and Na-ascorbate-sensitive effects on the PSII donor side reactions (59). This is because the presence of both DCMU and Na-ascorbate in all the experimental samples in this paper should have completely inhibited all PSII Chl *a* fluorescence quenching due to Δ pH-induced inhibition of the PSII donor side reactions (6,59).

The ideas that the xanthophyll cycle mechanism is an all or none reaction for individual PSII units (Fig. 5, lower right), while photoinhibition is a slower progressive decay (Fig. 5, lower left) are similar to those earlier reviewed by Krause (1), but this paper contains the first direct time-resolved confirmation of both these hypotheses. Our two-stage model for xanthophyll cycle-dependent nonphotochemical quenching is similar to the model proposed by Weis and Berry (60) to explain the effects of nonphotochemical fluorescence quenching on the quantum yield of PSII photochemistry. Further, our interpretations of the different effects of the xanthophyll cycle and photoinhibition mechanisms on the Chl *a* fluorescence lifetimes are consistent with the well-established different effects that these mechanisms have on the steady-state PSII Chl *a* fluorescence intensity parameters when PSII photochemistry and Q_A oxidation is not inhibited by DCMU (as they were in this study). It is firmly established that the xanthophyll cycle mechanism decreases the

minimal PSII Chl *a* fluorescence yield, F_o , when PSII photochemistry is at a maximum (when all Q_A is oxidized), in direct proportion to the maximal fluorescence yield, F_m , when PSII photochemistry is at a minimum (when all Q_A is reduced) (2,4–6,53). However, photoinhibition normally increases the F_o level while decreasing the F_m level (2,7,31–33). Indeed, the idea that the photoinhibition affects the charge-separated state of the reaction center (9,13, this paper) while the xanthophyll quenching affects the PSII antenna conformation and, thus energy delivery from the antenna to the P680 Chl (4–6, this paper), would according to all currently accepted models of PSII exciton kinetics, structure and function explain the different effects on F_o and F_m (see review by Dau (61)).

Acknowledgements—A.G. was supported by a training grant (DOE 92ER20095) from the Triagency (DOE/NSF/USDA) Program for Collaborative Research in Plant Biology. T.L.H. thanks NIH grant RR03155. We thank Drs. Barbara Demmig-Adams and William Adams III, their laboratory staff and graduate students for the use of their HPLC equipment and for stimulating discussions with regard to the subject of this manuscript. We thank Dr. D. Simpson of the Carlsberg Research Laboratories for the barley seeds and Ms. Purma Lakhia for her help in growing the plants and laboratory assistance.

REFERENCES

- Krause, G. H. (1988) Photoinhibition of photosynthesis. An evaluation of damaging and protective mechanisms. *Physiol. Plant.* **74**, 566–574.
- Osmond, C. B. (1994) What is photoinhibition? Some insights from comparisons of shade and sun plants. In *Photoinhibition of Photosynthesis* (Edited by N. R. Baker and J. R. Bowyer), pp. 1–24. Oxford Publishers, UK.
- Yamamoto, H. Y. and R. Bassi (1996) Carotenoids: localization and function. In *Oxygenic Photosynthesis: The Light Reactions. Advances in Photosynthesis* (Edited by D. R. Ort and C. F. Yocum), pp. 539–563. Kluwer Academic Publishers, Dordrecht.
- Demmig-Adams, B., A. M. Gilmore and W. W. Adams III (1996) *In vivo* functions of carotenoids in plants. *FASEB J.* **10**, 403–412.
- Horton, P., A. V. Ruban and R. G. Walters (1994) Regulation of light harvesting in green plants. *Plant Physiol.* **106**, 415–420.
- Gilmore, A. M., T. L. Hazlett and Govindjee (1995) Xanthophyll cycle dependent quenching of photosystem II chlorophyll *a* fluorescence: formation of a quenching complex with a short fluorescence lifetime. *Proc. Natl. Acad. Sci. USA* **92**, 2273–2277.
- Powles, S. B. (1984) Photoinhibition of photosynthesis induced by visible light. *Annu. Rev. Plant Physiol.* **35**, 15–44.
- Barber, J. (1995) Molecular basis of the vulnerability of photosystem II to damage by light. *Aust. J. Plant Physiol.* **22**, 167–181.
- Renger, G., H.-J. Eckert, A. Bergmann, J. Bernarding, B. Liu, A. Napiwotzki, F. Reifarth and H. J. Eichler (1995) Fluorescence and spectroscopic studies of exciton trapping and electron transfer in photosystem II of higher plants. *Aust. J. Plant Physiol.* **22**, 167–181.
- Andersson, B. and J. Barber (1996) Mechanisms of photodamage and protein degradation during photoinhibition of photosystem II. In *Photosynthesis and the Environment* (Edited by N. R. Baker). Kluwer Academic Publishers, Dordrecht, the Netherlands. (In press)
- Mishra, N. P., C. Francke, H. J. van Gorkom and D. F. Ghanotakis (1994) Destructive role of singlet oxygen during aerobic illumination of the photosystem II core complex. *Biochim. Biophys. Acta* **1186**, 81–90.
- Vass, I., G. Gatzzen and A. R. Holzwarth (1993) Picosecond time-resolved fluorescence studies on photoinhibition and double reduction of Q_A in photosystem II. *Biochim. Biophys. Acta* **1183**, 388–396.

13. Kirilovsky, D., W. A. Rutherford and A.-L. Etienne (1994) Influence of DCMU and ferricyanide on photodamage in photosystem II. *Biochemistry* **33**, 3087–3095.
14. Diner, B. A. and G. T. Babcock (1996) Structure, dynamics and energy conversion efficiency in photosystem II. In *Oxygenic Photosynthesis: The Light Reactions* (Edited by D. R. Ort and C. F. Yocum), pp. 213–247. Kluwer Academic Publishers, Dordrecht, the Netherlands.
15. Govindjee (1995) Sixty-three years since Kautsky: chlorophyll *a* fluorescence. *Aust. J. Plant Physiol.* **22**, 131–160.
16. Yamamoto, Y. and T. Akasaka (1995) Degradation of antenna chlorophyll-binding protein CP43 during photoinhibition of photosystem II. *Biochemistry* **34**, 9038–9045.
17. Hager, A. (1969) Lichtbedingte pH-Erniedrigung in einem Chloroplasten-Kompartiment als Ursache der enzymatischen Violaxanthin → Zeaxanthin-Umwandlung; Beziehungen zur Photophosphorylierung. *Planta* **89**, 224–243.
18. Yamamoto, H. Y., T. O. M. Nakayama and C. O. Chichester (1962) Studies on the light and dark interconversions of leaf xanthophylls. *Arch. Biochem. Biophys.* **97**, 168–173.
19. Jahns, P. and W. Junge (1990) Dicyclohexylcarbodiimide-binding proteins related to the short circuit of the proton-pumping activity of photosystem II. Identified as light-harvesting chlorophyll-*alb*-binding proteins. *Eur. J. Biochem.* **193**, 731–736.
20. Crofts, A. R. and C. T. Yerkes (1994) A molecular mechanism for q_E -quenching. *FEBS Lett.* **352**, 265–270.
21. Walters, R. G., A. V. Ruban and P. Horton (1994) Higher plant light-harvesting complexes LHClIa and LHClIc are bound by dicyclohexylcarbodiimide during inhibition of energy dissipation. *Eur. J. Biochem.* **226**, 1063–1069.
22. Bassi, R., B. Pineau, P. Dainese and J. Marquardt (1993) Carotenoid-binding proteins of photosystem II. *Eur. J. Biochem.* **212**, 297–303.
23. Jahns, P. and S. Schweig (1995) Energy-dependent fluorescence quenching in thylakoids from intermittent light grown pea plants—evidence for an interaction of zeaxanthin and the chlorophyll *alb* binding protein CP26. *Plant Physiol. Biochem.* **33**, 683–687.
24. Blubaugh, D. J., M. Atamian and G. T. Babcock (1991) Photoinhibition of hydroxylamine-extracted photosystem II membranes: identification of the sites of photodamage. *Biochemistry* **30**, 7586–7597.
25. Chen, G. X., D. J. Blubaugh, P. H. Homann, J. H. Golbeck and G. M. Cheniaie (1995) Superoxide contributes to the rapid inactivation of specific secondary donors of the photosystem II reaction center during photodamage of manganese-depleted photosystem II membranes. *Biochemistry* **34**, 2317–2332.
26. Vass, I., Y. Sanakis, C. Spetea and V. Petrouleas (1995) Effects of photoinhibition on the Q_A - Fe^{2+} complex of photosystem II studied by EPR and Mössbauer spectroscopy. *Biochemistry* **34**, 4434–4440.
27. Govindjee, M. Van de Ven, J. Cao, C. Royer and E. Gratton (1993) Multifrequency cross-correlation phase fluorometry of chlorophyll *a* fluorescence in thylakoid and PSII-enriched membranes. *Photochem. Photobiol.* **58**, 438–445.
28. Van Mieghem, F. J. E., G. F. W. Searle, A. W. Rutherford and T. J. Schaafsma (1992) The influence of double reduction of Q_A on the fluorescence decay kinetics of photosystem II. *Biochim. Biophys. Acta* **1100**, 198–206.
29. Gilmore, A. M., T. L. Hazlett, P. G. Debrunner and Govindjee (1996) Photosystem II chlorophyll *a* fluorescence lifetimes are independent of the antenna size differences between barley wild-type and *chlorina* mutants: comparison of xanthophyll-cycle dependent and photochemical quenching. *Photosynth. Res.* (In press)
30. Govindjee, M. Van de Ven, C. Preston, M. Seibert and E. Gratton (1990) Chlorophyll *a* fluorescence lifetime distributions in open and closed photosystem II reaction center preparations. *Biochim. Biophys. Acta* **1015**, 173–179.
31. Krause, G. H. and U. Behrend (1986) Δ pH-dependent chlorophyll fluorescence quenching indicating a mechanism of protection against photoinhibition of chloroplasts. *FEBS Lett.* **200**, 298–302.
32. Kyle, D. J. (1987) The biochemical basis for photoinhibition of photosystem II. In *Photoinhibition* (Edited by D. J. Kyle, C. B. Osmond and C. J. Arntzen), pp. 197–226. Elsevier Science Publishers, Amsterdam.
33. Bilger, W. and O. Björkman (1990) Role of the xanthophyll cycle in photoprotection elucidated by measurements of light-induced absorbance changes, fluorescence and photosynthesis in leaves of *Hedera canariensis*. *Photosynth. Res.* **25**, 173–185.
34. Graan, T. and D. R. Ort (1984) Quantitation of the rapid electron donors to P700, the functional plastoquinone pool, and the ratio of the photosystems in spinach chloroplasts. *J. Biol. Chem.* **22**, 14003–14010.
35. Porra, R. J., W. A. Thompson and P. E. Kriedmann (1989) Determination of accurate extinction coefficients and simultaneous equations for assaying chlorophylls *a* and *b* extracted with four different solvents: verification of the concentration of chlorophyll standards by atomic absorption spectroscopy. *Biochim. Biophys. Acta* **975**, 384–394.
36. Yamamoto, H. Y. and L. Kamite (1972) The effects of dithiothreitol on violaxanthin de-epoxidation and absorbance changes in the 500-nm region. *Biochim. Biophys. Acta* **267**, 538–543.
37. Petrack, B. and F. Lipman (1961) Photophosphorylation and photohydrolysis in cell-free preparations of blue-green algae. In *Light and Life* (Edited by W. D. Mc Elroy and B. Glass), pp. 621–630. Johns Hopkins Press, Baltimore.
38. Mills, J. D. and P. Mitchell (1982) Modulation of coupling factor ATPase activity in intact chloroplasts. Reversal of thiol modulation in the dark. *Biochim. Biophys. Acta* **679**, 75–83.
39. Gilmore, A. M. and H. Y. Yamamoto (1991) Resolution of lutein and zeaxanthin using a nonendcapped, lightly carbon-loaded C-18 high-performance liquid chromatographic column. *J. Chromatogr.* **543**, 137–145.
40. Frauenfelder, H., F. Parak and R. D. Young (1988) Conformational substates in proteins. *Annu. Rev. Biophys. Biophys. Chem.* **17**, 451–479.
41. Schatz, G. H., H. Brock and A. R. Holzwarth (1988) A kinetic and energetic model for the primary processes in photosystem II. *Biophys. J.* **54**, 397–405.
42. Pearlstein, R. M. (1982) Chlorophyll singlet excitons. In *Photosynthesis: Energy Conversion by Plants and Bacteria* (Edited by Govindjee), pp. 294–391. Academic Press, New York.
43. Kudzmauskas, S., L. Valkunas and A. Y. Borisov (1983) A theory of excitation transfer in photosynthetic units. *J. Theor. Biol.* **105**, 13–23.
44. Jennings, R. C., R. Bassi, F. M. Garlaschi, P. Dainese and G. Zucchelli (1993) Distribution of the chlorophyll spectral forms in the chlorophyll–protein complexes from photosystem II. *Biochemistry* **32**, 3203–3210.
45. Dau, H. and K. Sauer (1996) Exciton equilibration and photosystem II exciton dynamics—a fluorescence study on photosystem II membrane particles of spinach. *Biochim. Biophys. Acta* **1273**, 175–190.
46. Briantais, J.-M., J. Dacosta, Y. Goulas, J.-M. Ducruet and I. Moya (1996) Heat-stress induces in leaves an increase of the minimum level of chlorophyll fluorescence, F_o ; a time-resolved fluorescence analysis. *Photosynth. Res.* (In press)
47. Lin, S. and R. S. Knox (1991) Studies of excitation energy transfer within the green alga *Chlamydomonas reinhardtii* and its mutants at 77 K. *Photosynth. Res.* **27**, 157–168.
48. Knoetzel, J. and D. Simpson (1991) Expression and organization of antenna proteins in the light- and temperature-sensitive barley mutant *chlorina*⁻¹⁰⁴. *Planta* **185**, 111–123.
49. Gilmore, A. M. and H. Y. Yamamoto (1993) Linear models relating xanthophylls and lumen acidity to non-photochemical fluorescence quenching. Evidence that antheraxanthin explains zeaxanthin-independent quenching. *Photosynth. Res.* **35**, 67–78.
50. Jahns, P. (1995) The xanthophyll cycle in intermittent light-grown pea plants. *Plant Physiol.* **108**, 149–156.
51. Goss, R., M. Richter and A. Wild (1995) Role of Δ pH in the mechanism of zeaxanthin-dependent amplification of q_E . *J. Photochem. Photobiol.* **27**, 147–152.
52. Härtel, H. and H. Lokstein (1995) Relationship between quenching of maximum and dark-level chlorophyll fluorescence *in vivo*: dependence on photosystem II antenna size. *Biochim. Biophys. Acta* **1228**, 91–94.

53. Gilmore, A. M. and H. Y. Yamamoto (1992) Dark induction of zeaxanthin-dependent nonphotochemical fluorescence quenching mediated by ATP. *Proc. Natl. Acad. Sci. USA* **89**, 1899–1903.
54. Jeffrey, S. W., R. Douce and A. A. Benson (1974) Carotenoid transformations in the chloroplast envelope. *Proc. Natl. Acad. Sci. USA* **71**, 807–810.
55. Siefermann-Harms, D., J. Joyard and R. Douce (1978) Light-induced changes of the carotenoid levels in chloroplast envelopes. *Plant Physiol.* **61**, 530–533.
56. Siefermann, D. and H. Y. Yamamoto (1976) Light-induced de-epoxidation in lettuce chloroplasts. VI. De-epoxidation in grana and stroma lamellae. *Plant Physiol.* **57**, 939–940.
57. Lee, A. L. and J. P. Thornber (1995) Analysis of the pigment stoichiometry of pigment–protein complexes from barley (*Hordeum vulgare*). *Plant Physiol.* **107**, 565–574.
58. Thayer, S. S. and O. Björkman (1992) Carotenoid distribution and deepoxidation in thylakoid pigment–protein complexes from cotton leaves and bundle-sheath cells of maize. *Photosynth. Res.* **33**, 213–225.
59. Krieger, A., I. Moya and E. Weis (1992) Energy-dependent quenching of chlorophyll *a* fluorescence: effect of pH on stationary fluorescence and picosecond-relaxation kinetics in thylakoid membranes and photosystem II preparations. *Biochim. Biophys. Acta* **1102**, 167–176.
60. Weis, E. and J. A. Berry (1987) Quantum efficiency of photosystem II in relation to 'energy'-dependent quenching of chlorophyll fluorescence. *Biochim. Biophys. Acta* **894**, 198–207.
61. Dau, H. (1994) Molecular mechanisms and quantitative models of variable photosystem II fluorescence. *Photochem. Photobiol.* **60**, 1–23.